



# IMAGGarment-1: Fine-Grained Garment Generation for Controllable Fashion Design

Fei Shen<sup>1</sup>, Jian Yu<sup>1</sup>, Cong Wang<sup>2</sup>, Xin Jiang<sup>1</sup>, Xiaoyu Du<sup>1</sup>, Jinhui Tang<sup>1</sup>

<sup>1</sup>Nanjing University of Science and Technology

<sup>2</sup>Nanjing University

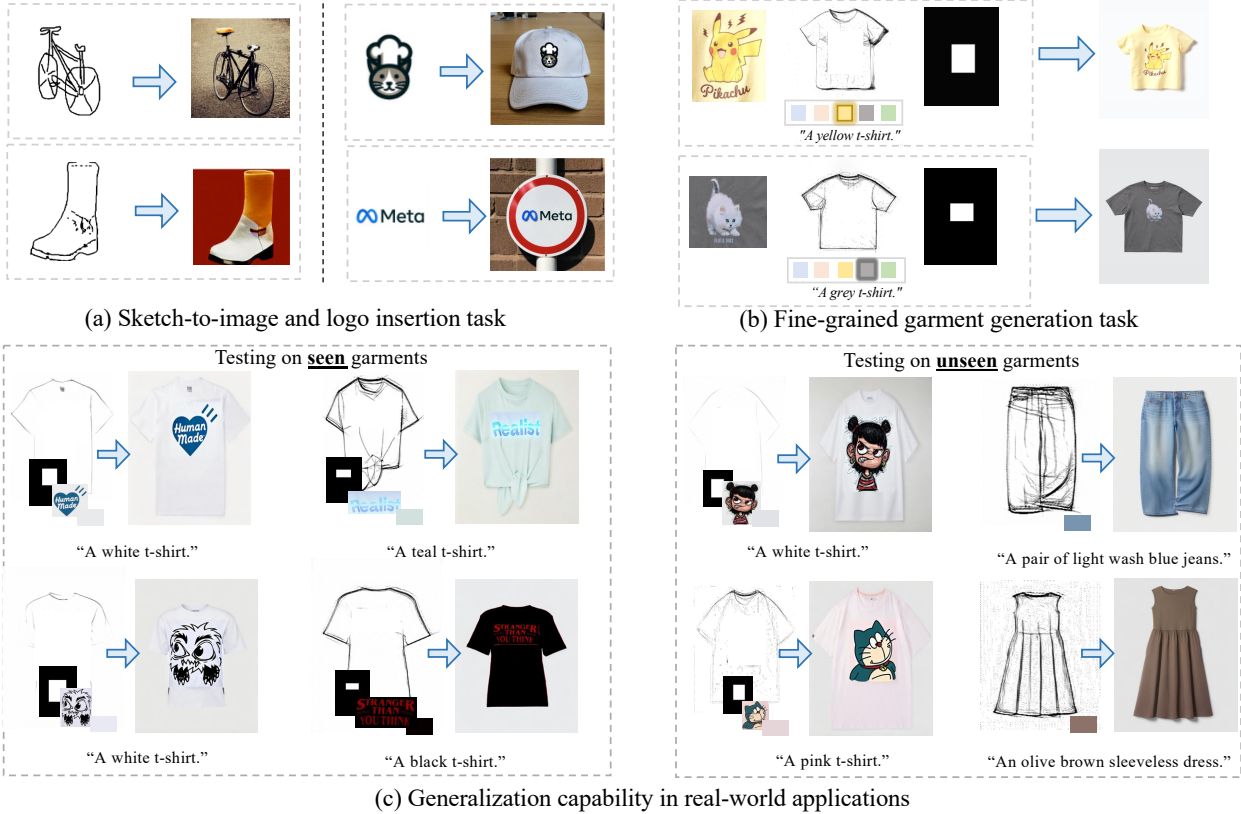


**Figure 1: Comparison of (a) existing sketch-to-image and logo insertion tasks with (b) our proposed fine-grained garment generation (FGG) task, which enables precise and controllable synthesis of garment structure, color, logo, and spatial placement. Unlike previous tasks that rely on a single input condition, FGG is tailored for real-world fashion design workflows by integrating multiple conditional controls.**

## ABSTRACT

This paper presents IMAGGarment-1, a fine-grained garment generation (FGG) framework that enables high-fidelity garment synthesis with precise control over silhouette, color, and logo placement. Unlike existing methods that are limited to single-condition inputs, IMAGGarment-1 addresses the challenges of multi-conditional controllability in personalized fashion design and digital apparel applications. Specifically, IMAGGarment-1 employs a two-stage training strategy to separately model global appearance and local details, while enabling unified and controllable generation through end-to-end inference. In the first stage, we propose a global appearance model that jointly encodes silhouette and color using a mixed attention module and a color adapter. In the second stage, we present a local enhancement model with an adaptive appearance-aware module to inject user-defined logos and spatial constraints, enabling

accurate placement and visual consistency. To support this task, we release GarmentBench, a large-scale dataset comprising over 180K garment samples paired with multi-level design conditions, including sketches, color references, logo placements, and textual prompts. Extensive experiments demonstrate that our method outperforms existing baselines, achieving superior structural stability, color fidelity, and local controllability performance. The code and model are available at <https://github.com/muzishen/IMAGGarment-1>.

## CCS CONCEPTS

• Human-centered computing → Visualization design and evaluation methods.

## KEYWORDS

Fine-Grained Garment Generation; Multi-Conditional Generation; Fashion Design Applications; GarmentBench Dataset

## 1 INTRODUCTION

Fine-Grained garment generation (FGG) aims to synthesize high-quality garments with precise control over garment silhouette, color scheme, logo content, and spatial placement. As personalized fashion and the digital apparel market grow rapidly, fine-grained controllability is increasingly crucial for applications in fashion design, brand customization, and personalized e-commerce.

Recently, image synthesis [26, 33] has made notable progress in tasks such as sketch-to-image generation [19, 39] and logo insertion [21] (as illustrated in Figure 1 (a)), demonstrating basic capabilities in structural and content-level control. However, these tasks provide only coarse guidance and rely on single-condition inputs (e.g., sketch or color), lacking the fine-grained controllability needed to model the nuanced interactions between global structure and local details in garment design. Although sequential or modular combinations may offer partial solutions, they fail to explicitly disentangle and jointly model global attributes (e.g., silhouette, color) and local appearance details (e.g., logo content and spatial placement). Without unified control mechanisms or hierarchical representations, these approaches often suffer from condition entanglement, conflicting objectives, and visual inconsistencies, ultimately falling short of the high standards required in real-world fashion design. In contrast, practical fashion design requires joint control over multiple interdependent factors: designers determine global attributes such as silhouette and color, followed by fine-tuning of local elements like logos and their placement. To support this process, a unified generation task that clearly separates and coordinates global and local attributes is essential for controllable and high-fidelity synthesis.

To address these limitations, we propose a new task: fine-grained garment generation (FGG), as illustrated in Figure 1 (b). FGG is formulated as a unified multi-conditional garment synthesis task, taking a textual prompt, garment silhouette, color palette, and spatially constrained logos as joint inputs. It aims to generate garments that faithfully reflect high-level structural intent and fine-grained local styling cues. FGG is specifically designed to mirror real-world fashion workflows, where designers must coordinate diverse input modalities to express creative intent. Unlike conventional approaches that process each condition independently or sequentially, FGG emphasizes joint modeling and hierarchical reasoning across input types. It goes beyond simple task combinations by enforcing consistent integration of global and local attributes within a unified generation framework, enabling nuanced control over the overall structure and detailed appearance. Specifically, **FGG task introduces three key challenges**: (1) maintaining visual and semantic consistency across heterogeneous input conditions, (2) resolving conflicts between global structures and localized visual elements, and (3) generalizing to unseen condition combinations without retraining (see Figure 1(c)). FGG thus marks a fundamental shift from single-condition or loosely coupled pipelines toward a unified, design-intent-driven generation paradigm that better reflects the complexity of real-world garment design.

To this end, we propose IMAGGarment-1, a two-stage training and end-to-end inference framework tailored for fine-grained garment generation. Unlike prior methods [34, 42, 45] that rely on single-condition inputs or simple feature fusion, our framework is explicitly designed to achieve fine-grained controllability under multiple, interdependent constraints. In the first stage, we propose a global appearance model with a mixed attention module and a color adapter to jointly encode garment silhouette and color palette, improving overall appearance fidelity and mitigating condition entanglement. In the second stage, we present a local enhancement model equipped with an adaptive appearance-aware module to inject user-defined logos and their spatial constraints, enabling precise logo placement while preserving global consistency. To further promote research in this direction, we release GarmentBench, a large-scale dataset comprising over 180k garment samples annotated with rich multi-level design conditions, including silhouette sketches, color references, logo placements, and textual prompts. Extensive experiments demonstrate that IMAGGarment-1 significantly outperforms existing baselines in terms of structural stability and local controllability. To summarize, the main contributions are listed as follows:

- We propose IMAGGarment-1, a controllable garment generation framework that enables precise control over garment structure, color, and logo placement, addressing the challenges of FGG.
- We design a mixed attention module, color adapter, and adaptive appearance-aware module to disentangle global structure from local attributes, achieving fine-grained visual control and accurate spatial control.
- We release GarmentBench, a large-scale dataset with diverse garments and rich multi-conditional annotations, serving as a valuable benchmark for FGG research.

## 2 RELATED WORK

### 2.1 GAN-Based Methods

Early approaches [3, 4, 6, 13, 13, 24, 40] to garment generation often employ generative adversarial networks (GANs) [9, 31, 32], focusing primarily on sketch-to-image translation [27] by learning spatial mappings from structural cues. For example, DeepFaceDrawing [4] and DeepFaceEditing [3] decompose sketches into individual facial components and progressively assemble them into photorealistic portraits. Then, DeepPortraitDrawing [40] extends this strategy to full-body synthesis using a local-to-global pipeline. Similarly, Interactive frameworks [13] introduce gating mechanisms to support user-driven editing, while DALColor [8] combines WGAN-GP with line-art colorization for refined appearance control. However, these methods [3, 4, 13, 40] are limited to single-condition generation and are difficult to apply in real-world fashion scenarios that demand multi-conditional controllability. Moreover, GAN-based approaches [29, 31, 36] are prone to adversarial training instability and image artifacts, often compromising realism.

### 2.2 Diffusion-Based Methods

Diffusion models [12, 17, 38] have made significant strides in conditional image generation, thanks to their iterative denoising mechanism and flexible control capacity. To enhance controllability,



plugin-based methods such as IP-Adapter [42], ControlNet [45], and BLIP-Diffusion [23] inject external conditions into pre-trained diffusion models via lightweight modules. Parallel architectures [5, 25, 35, 41] further improve control precision by incorporating reference-guided features during generation. In the fashion domain, Diff-Cloth [47] enables localized garment editing via part-specific textual prompts, allowing independent control over different regions (e.g., sleeves, collars). For logo generation, AnyLogo [44] employs a dual-state denoising strategy to preserve fine logo details; Lo-goSticker [48] introduces token-based injection for flexible logo placement; and RefDiffuser [21] leverages expert-driven plugins to enhance texture and spatial fidelity. However, these methods typically focus on either global appearance or localized editing in isolation, and lack a unified framework for jointly modeling multiple design conditions in fine-grained garment synthesis.

### 3 METHODOLOGY

**Task Definition.** Given a garment silhouette, color palette, user-defined logo, location and an optional text description, fine-grained garment generation (FGG) aims to synthesize high-fidelity garment images with precise control over both global structure and local visual attributes. The key challenges lie in jointly modeling multi-conditional inputs, maintaining semantic and visual consistency across different design factors, and supporting controllable placement of fine-grained elements such as logos and color regions.

#### 3.1 Overall Framework

To address the above challenges, we propose IMAGGarment-1, a conditional diffusion framework tailored for fine-grained garment generation. Our framework comprises two components: a global appearance model (stage I) and a local enhancement model (stage II), which explicitly disentangle and jointly control the global appearance and local details under multi-conditional guidance, enabling accurate synthesis of garment silhouette, color, and logo placement. As illustrated in Figure 2, the global appearance model first generates a latent of coarse garment image conditioned on the textual prompt, garment silhouette, and color palette. Subsequently, the local enhancement model refines this latent representation by integrating user-defined logo and spatial constraint, producing the final high-fidelity garment image with fine-grained controllability. Specifically, the global appearance model (Section 3.2) leverages our proposed mixed attention module and color adapter to effectively capture global appearance features from textual descriptions, silhouettes, and colors, while mitigating entanglement among these conditions. The local enhancement model (Section 3.3) introduces an adaptive appearance-aware module ( $A^3$  Module) that injects logo content and spatial location constraint into the latent space, achieving precise logo placement. Finally, the training and inference strategies used in IMAGGarment-1 are summarized in Section 3.4.

#### 3.2 Stage I: Global Appearance Model

**Motivation.** Existing garment generation methods [34, 42, 45] typically rely on single-condition inputs (e.g., sketch or text), causing entangled features and limited controllability. To resolve this, we propose a global appearance model that explicitly disentangles silhouette, color, and text, enabling precise multi-conditional control.

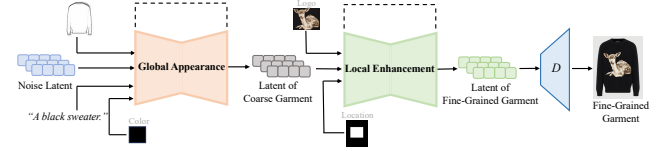


**Figure 2: Visualization of the IMAGGarment-1 inference pipeline.** The global appearance model generates coarse latent from textual prompts, silhouettes, and colors. The local enhancement model then injects user-defined logos and spatial location constraints to produce the fine-grained garment.

**Architecture.** As shown in the left of the Figure 3, our global appearance model comprises two shared frozen VAE encoders, one frozen VAE decoder, a trainable silhouette UNet, a frozen text encoder, a trainable color adapter, and a denoising UNet with the proposed mixed attention. Specifically, we first utilize the frozen VAE encoder to project the input reference silhouette into the latent space. Subsequently, we employ a trainable silhouette UNet (structurally identical to the denoising UNet but without cross attention) to extract fine-grained silhouette features, which are then integrated into the frozen denoising UNet via our proposed mixed attention module. Meanwhile, textual features obtained from the frozen CLIP text encoder and color features extracted by the proposed color adapter are further fused into the denoising UNet through cross attention. After multiple denoising iterations, the model generates coarse garment images that precisely align with the reference silhouette and faithfully reflect user-specified color.

**Mixed Attention.** To effectively incorporate reference silhouette features into the denoising UNet without compromising the generative capability of the original UNet, we propose a mixed attention module. As shown in Figure 3, we extend all self attention layers in the denoising UNet to the proposed mixed attention, which introduces two additional learnable projection layers to align the silhouette features  $C_s$  with the latent features  $Z_t$ . Formally, the mixed attention is defined as:

$$Z_m = \text{Softmax} \left( \frac{QK^T}{\sqrt{d}} \right) V + \alpha \cdot \text{Softmax} \left( \frac{Q(K')^T}{\sqrt{d}} \right) V', \quad (1)$$

where  $\alpha$  is a hyperparameter controlling the strength of silhouette conditioning. The projections are computed as follows:

$$Q = Z_t W_q, K = Z_t W_k, V = Z_t W_v, K' = C_s W'_k, V' = C_s W'_v \quad (2)$$

where  $W_q, W_k, W_v$  are frozen parameters of linear projection layers, whereas  $W'_k, W'_v$  are newly introduced learnable parameters of projection layers initialized from  $W_k$  and  $W_v$ , respectively. Our mixed attention facilitates the seamless integration of silhouette features into the denoising UNet, thus ensuring that generated garments maintain precise spatial alignment with the reference silhouette.

**Color Adapter.** Accurate color manipulation is essential for generating garments with fine-grained visual details, significantly enhancing visual quality and realism. However, as the base model's textual prompts cannot reliably produce the intended colors, discrepancies often arise between the generated and expected colors. To address this issue, we propose a dedicated color adapter that explicitly treats color as an independent controllable factor. Specifically, given a reference color image, we extract color features  $C_c$

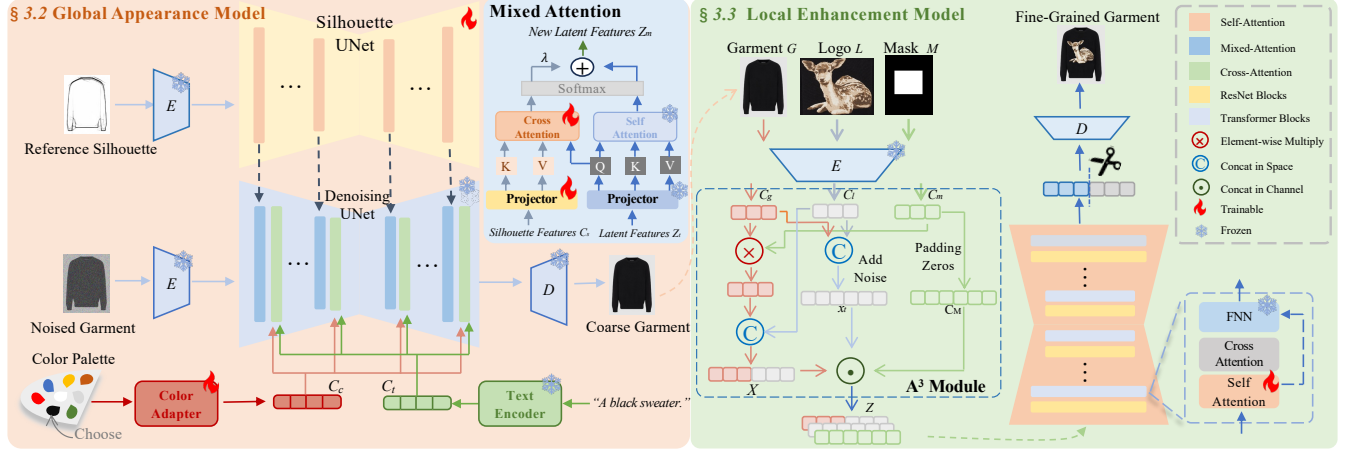


**Figure 3: Overview of our IMAGGarment-1 framework.** IMAGGarment-1 is a two-stage conditional diffusion framework for fine-grained garment generation. The global appearance model first synthesizes a coarse latent representation from the input text prompt, silhouette, and color palette using a parallel UNet with mixed attention and a color adapter. The local enhancement model then refines this latent by injecting user-defined logos and location constraints through the proposed  $A^3$  module, enabling precise logo placement and high-fidelity garment generation.

using a frozen CLIP image encoder combined with a trainable linear layer. Subsequently, these color features are integrated into the denoising UNet via a cross attention mechanism, jointly with textual features  $C_t$  obtained from the frozen CLIP text encoder:

$$Z_{new} = \text{Softmax} \left( \frac{QK_t^T}{\sqrt{d}} \right) V_t + \beta \cdot \text{Softmax} \left( \frac{QK_c^T}{\sqrt{d}} \right) V_c, \quad (3)$$

where  $Q = Z_t W_q$ ,  $K_t = C_t W_k^t$ ,  $V_t = C_t W_v^t$ , and  $K_c = C_c W_k^c$ ,  $V_c = C_c W_v^c$ . Here,  $W_k^t$ ,  $W_v^t$  denote frozen parameters of the original cross attention layers in the denoising UNet, while  $W_k^c$ ,  $W_v^c$  are newly introduced trainable projection layers. The hyperparameter  $\beta$  modulates the adapter's influence, ensuring precise alignment between generated colors and user specifications.

### 3.3 Stage II: Local Enhancement Model

**Motivation.** Existing methods [44, 48] typically neglect detailed logo integration or treat it as a separate task, causing poor spatial alignment and visual inconsistency. To address this limitation, we propose a local enhancement model equipped with an adaptive appearance-aware ( $A^3$ ) module, explicitly injecting user-defined logos and spatial constraints into the latent space. This design enables precise, consistent control over localized garment details, significantly enhancing visual fidelity.

**Architecture.** As illustrated on the right of Figure 3, the local enhancement model comprises a frozen VAE encoder and decoder, a denoising UNet, and an adaptive appearance-aware module ( $A^3$  module). The  $A^3$  module fuses local conditions, such as logos and spatial constraints, by concatenating them along spatial or channel dimensions, enabling precise control over fine-grained visual elements. Given a garment, logo, and placement mask, the model adaptively adjusts the logo's size and position while preserving its visual fidelity. To reduce redundancy and focus on local detail

refinement, we optimize only the self attention layers of the denoising UNet and discard all cross attention layers, as the global appearance model has already encoded the textual information.

**$A^3$  Module.** To precisely integrate fine-grained logo details into designated garment regions, we introduce the adaptive appearance-aware ( $A^3$ ) module. By fusing image-based conditions across specific dimensions, our  $A^3$  module enables precise and consistent logo integration. Specifically, given a coarse garment image  $G$ , a logo image  $L$ , and a binary placement mask  $M$ , we first encode them using a frozen VAE encoder to obtain their corresponding latent features:  $C_g \in \mathbb{R}^{4 \times \frac{H}{8} \times \frac{W}{8}}$  and  $C_l \in \mathbb{R}^{4 \times \frac{H}{8} \times \frac{W}{8}}$ . The mask  $M$  is resized via nearest-neighbor interpolation to match the latent resolution, resulting in  $C_m \in \mathbb{R}^{1 \times \frac{H}{8} \times \frac{W}{8}}$ . We then construct the spatially aligned conditional input as:

$$X = \text{Concat}(C_g \otimes C_m, C_l), \quad X \in \mathbb{R}^{4 \times \frac{H}{8} \times \frac{W}{4}}, \quad (4)$$

where  $\otimes$  denotes element-wise multiplication and  $\text{Concat}$  indicates spatial concatenation along the width dimension. To align with  $X$ , the resized mask  $C_m$  is zero-padded to obtain  $C_M \in \mathbb{R}^{1 \times \frac{H}{8} \times \frac{W}{4}}$ . Next, we concatenate the garment and logo features to form a clean latent representation:

$$x_0 = \text{Concat}(C_g, C_l), \quad (5)$$

and inject noise consistent with the diffusion process:

$$x_t = \sqrt{\bar{\alpha}_t} \cdot x_0 + \sqrt{1 - \bar{\alpha}_t} \cdot \epsilon, \quad \epsilon \sim \mathcal{N}(0, \mathbf{I}), \quad (6)$$

where  $x_0$  denotes the clean latent feature obtained by concatenating garment and logo features, and  $x_t \in \mathbb{R}^{4 \times \frac{H}{8} \times \frac{W}{4}}$  is the corresponding noisy latent at diffusion timestep  $t$ .  $\bar{\alpha}_t$  is the cumulative product of the noise schedule coefficients, and  $\epsilon$  is the Gaussian noise sampled from  $\mathcal{N}(0, \mathbf{I})$ . Finally, the full model input is obtained by concatenating the noisy latent  $x_t$ , the padded mask  $C_M$ , and the aligned conditional input  $X$  along the channel dimension:

$$Z = \text{Concat}(x_t, C_M, X), \quad Z \in \mathbb{R}^{9 \times \frac{H}{8} \times \frac{W}{4}}. \quad (7)$$





This channel-wise concatenation allows the model to jointly reason over appearance, spatial constraints, and guidance signals, while maintaining compatibility with the UNet architecture for spatially aware logo synthesis.

### 3.4 Training and Inference

**Training.** The training process is divided into two stages, each targeting a specific set of objectives with separate optimization strategies. Both stages adopt mean squared error (MSE) loss to supervise the denoising process.

**Stage I.** The global appearance model  $\epsilon_{\theta_g}$  is trained to synthesize garments that align with the target silhouette and color under textual guidance. To preserve the generative capacity of the pretrained denoising UNet, we freeze all parameters except those of the silhouette UNet and the cross-attention projections in the mixed attention module. Given silhouette features  $C_s$ , text embeddings  $C_t$ , and color features  $C_c$ , we adopt a decoupled training strategy with  $L_{\text{silhouette}}$  and  $L_{\text{color}}$  losses:

$$L_{\text{silhouette}} = \mathbb{E}_{x_0, \epsilon, C_t, C_s, t} \left\| \epsilon - \epsilon_{\theta_g}(x_t, C_t, C_s, t) \right\|^2, \quad (8)$$

$$L_{\text{color}} = \mathbb{E}_{x_0, \epsilon, C_t, C_c, t} \left\| \epsilon - \epsilon_{\theta_g}(x_t, C_t, C_c, t) \right\|^2,$$

where  $\epsilon$  is the added noise and  $\epsilon_{\theta_g}$  is the prediction from the global appearance model at timestep  $t$ .

**Stage II.** The local enhancement model  $\epsilon_{\theta_l}$  refines the coarse latent by injecting logos at user-defined locations. To reduce overhead, we fine-tune only the self-attention layers of the logo UNet. Given logo feature  $C_l$ , spatial mask  $C_m$ , and garment latent  $C_g$ , the training objective  $L_{\text{logo}}$  is:

$$L_{\text{logo}} = \mathbb{E}_{x_0, \epsilon, C_l, C_m, C_g, t} \left\| \epsilon - \epsilon_{\theta_l}(x_t, C_l, C_m, C_g, t) \right\|^2, \quad (9)$$

where  $\epsilon_{\theta_l}$  denotes the prediction from the local enhancement model.

**Inference.** IMAGGarment-1 supports end-to-end inference through a two-stage pipeline operating in a shared latent space. The global appearance model first generates a latent of coarse garment image conditioned on the input text prompt, silhouette, color, and mask. This process is guided by classifier-free guidance (CFG) [18]:

$$\tilde{\epsilon}_{\theta_g}(x_t, C_t, C_s, C_c, t) = w \cdot \epsilon_{\theta_g}(x_t, C_t, C_s, C_c, t) + (1 - w) \cdot \epsilon_{\theta_g}(x_t, t), \quad (10)$$

here,  $w$  is the CFG scale and  $x_t$  denotes the noisy latent at timestep  $t$ . The coarse latent is then refined by the local enhancement model, which incorporates user-defined logos and spatial constraints through the  $A^3$  module. We apply conditional CFG:

$$\tilde{\epsilon}_{\theta_l}(x_t, C_l, C_m, C_g, t) = w \cdot \epsilon_{\theta_l}(x_t, C_l, C_m, C_g, t) + (1 - w) \cdot \epsilon_{\theta_l}(x_t, C_m, C_g, t). \quad (11)$$

## 4 EXPERIMENTS

### 4.1 Dataset and Metrics

**Dataset Construction.** As shown in Figure 4 (a), we construct and release GarmentBench, a large-scale dataset for fine-grained garment generation, containing multi-modal design conditions such as text, sketches, colors, logos, and location masks. It serves as a controllable and extensible benchmark for advancing personalized fashion generation. The construction process is as follows:

**(1) Image Collection and Preprocessing.** We collect over 189K high-quality garment images from the internet, covering a wide

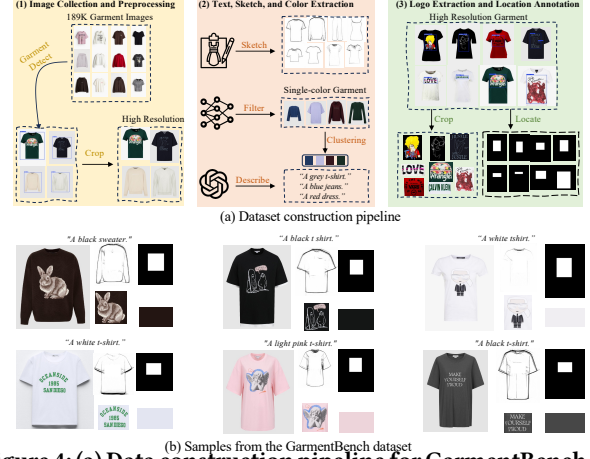


**Figure 4: (a) Data construction pipeline for GarmentBench. (b) Example samples with multimodal annotations: silhouette, logo, text, logo location, and color.**

range of categories such as tops, bottoms, and dresses. To eliminate background distractions and focus on the garment region, we apply YOLOv8 [20] for clothing detection and perform tight cropping to obtain clean garment-centric images for further processing.

**(2) Text, Sketch, and Color Extraction.** For each image, we automatically generate three auxiliary conditions to simulate real-world design guidance: textual descriptions generated by the multi-modal LLM Qwen-VL-Chat [1], covering key attributes such as color, silhouette, and style; structural sketches obtained using Informative Drawings [2], providing shape and layout priors; and color palettes extracted from single-color garments identified via ResNet50 [14] and clustered using K-means [30].

**(3) Logo Extraction and Location Annotation.** To support logo insertion and spatial control, we further extract local design elements such as logos and prints. We use YOLOv8 to detect visually distinct regions (e.g., anime characters, animal patterns), followed by manual verification to ensure label quality. We also annotate spatial locations and generate binary masks to serve as precise spatial constraints. In total, GarmentBench contains 189,966 garment-condition pairs with rich fine-grained annotations.

As shown in Figure 4 (b), we present representative samples from the GarmentBench dataset, which include fine-grained garment images paired with multi-modal conditions such as textual descriptions, structural silhouettes, color references, logos, and spatial location masks. Additionally, we randomly sample images from the Fashion-ControlNet-Dataset-V3<sup>1</sup> and apply the same preprocessing pipeline as GarmentBench to construct a test set with 1,267 image-condition pairs for evaluation and comparative analysis.

**Evaluation Metrics.** We adopt five metrics to comprehensively evaluate visual quality, conditional consistency, and fine-grained controllability. Fréchet inception distance (FID) [16] measures the distribution similarity between generated and real images, reflecting overall realism. Learned perceptual image patch similarity (LPIPS) [46] reflects human-perceived visual similarity, effectively capturing structural and textural consistency. Color structure similarity (CSS) [43] assesses the consistency of color distribution, measuring color controllability. Logo location accuracy (LLA) [11]

<sup>1</sup>[https://huggingface.co/datasets/Abrumu/Fashion\\_controlnet\\_dataset\\_V3](https://huggingface.co/datasets/Abrumu/Fashion_controlnet_dataset_V3)

quantifies the spatial deviation between generated and target logo positions, reflecting spatial precision. Lastly, CLIPScore [15] measures semantic alignment between the generated image and the input text prompt. These metrics comprehensively assess quality, controllability, and semantic alignment in fine-grained garment generation. See supplementary material for computational details.

## 4.2 Implementation Details.

In our experiments, both the silhouette UNet and the denoising UNet are initialized with the pretrained Stable Diffusion v1.5 model<sup>2</sup>. The local enhancement model is based on the inpainting variant of Stable Diffusion v1.5<sup>3</sup>, with only the self-attention layers being fine-tuned to reduce computational cost. We adopt OpenCLIP ViT-H/14<sup>4</sup> as the CLIP image encoder. All input images are resized to  $512 \times 640$  resolution. We use the AdamW optimizer [28] with a constant learning rate of  $1 \times 10^{-5}$ . The global appearance model and the local enhancement model are trained for 150K and 50K steps, respectively, using a batch size of 20. During inference, we adopt the DDIM sampler [37] with 50 sampling steps. Unless otherwise specified, the silhouette weight  $\alpha$  and color weight  $\beta$  in Eq.1 and Eq.3 are set to 0.6 and 1.0. The classifier-free guidance (CFG) scale  $w$  in Eq.10 and Eq.11 is set to a default value of 7.0.

## 4.3 Baseline Comparisons

Due to the absence of prior work tailored to fine-grained garment generation with multi-condition control, we compare our method against four representative baselines: BLIP-Diffusion [23], AnyDoor [7], ControlNet [45], and IP-Adapter [42]. For subject-driven generation methods, BLIP-Diffusion [23] leverages a learnable Q-Former to align textual and visual embeddings in the latent space, initially designed for subject-preserving generation from text-image pairs. AnyDoor [7] combines identity and detail encoders to reconstruct personalized content, which we adapt to conditions of garment appearance and logo inputs. For plugin-based baselines, we extend ControlNet [45] and IP-Adapter [42] by duplicating and modifying their conditional branches to support multi-conditional inputs, such as silhouette, color, and logo. The adapted versions are referred to as ControlNet-Garment and IP-Adapter-Garment. To ensure task relevance, all methods are fine-tuned on our GarmentBench dataset with support for logo-specific conditioning. All methods are trained and evaluated under identical training protocols, input resolutions, and hardware setups. The corresponding quantitative and qualitative results are presented in Table 1 and Figure 5, respectively, with detailed analysis provided below.

**Quantitative Results.** As shown in Table 1, IMAGGarment-1 achieves the best performance across all five metrics on the GarmentBench dataset, demonstrating its superiority in controllable fine-grained garment generation. Compared to subject-driven methods (BLIP-Diffusion [23], AnyDoor [7]), which rely on global features for personalized reconstruction, IMAGGarment-1 shows substantial improvements in FID, LPIPS, and CSS. These gains highlight the effectiveness of our mixed attention and color adapter modules

**Table 1: Quantitative comparisons on GarmentBench. Ours achieves the top results across all metrics, with best in bold.**

| Method                      | FID ↓          | LPIPS ↓       | CSS ↓          | LLA ↑         | CLIPScore ↑   |
|-----------------------------|----------------|---------------|----------------|---------------|---------------|
| BLIP-Diffusion* [23]        | 92.5187        | 0.6766        | 104.8677       | 0.1677        | 0.3144        |
| AnyDoor* [7]                | 60.0643        | 0.1728        | 46.6839        | 0.7487        | 0.2836        |
| ControlNet-Garment* [45]    | 31.7169        | 0.3978        | 82.0181        | 0.5304        | 0.3449        |
| IP-Adapter-Garment* [42]    | 24.5061        | 0.3416        | 76.4631        | 0.6609        | 0.3295        |
| <b>IMAGGarment-1 (Ours)</b> | <b>11.7038</b> | <b>0.0904</b> | <b>33.1443</b> | <b>0.7336</b> | <b>0.3460</b> |

\* denotes re-implemented by us for a fair comparison.

in achieving coherent multi-condition fusion, resulting in more realistic, perceptually consistent, and color-faithful outputs. In contrast to plugin-based approaches (ControlNet-Garment [45], IP-Adapter-Garment [42]) that simply stack independent conditional branches, IMAGGarment-1 yields significantly higher LLA and CLIPScore, reflecting more precise logo placement and stronger semantic-text alignment. Our proposed  $A^3$  module drives these improvements, which adaptively injects spatial priors and logo features into the latent space for accurate local control. Overall, these results indicate that global-only conditioning or naive plugin stacking is insufficient for fine-grained control. By contrast, IMAGGarment-1 provides an effective solution for multi-conditional garment synthesis, enabling precise coordination of global structure and local detail.

**Qualitative Results.** Figure 5 presents qualitative comparisons on both seen and unseen garments. Notably, the seen test set refers to the designated test split of our GarmentBench dataset. To assess generalization, we construct an unseen test set by randomly recombining input conditions (e.g., silhouette, color, logo) to simulate real-world fashion design scenarios. On seen garments, subject-driven methods (BLIP-Diffusion [23], AnyDoor [7]) reconstruct global appearance but lack spatial control. BLIP-Diffusion retains logo identity yet fails at precise placement due to text-only conditioning, while AnyDoor introduces logo distortions and stylistic artifacts. Plugin-based baselines (ControlNet-Garment [45], IP-Adapter-Garment [42]) treat conditions independently, resulting in poor coordination. ControlNet-Garment suffers from cross-condition interference, and IP-Adapter-Garment often misplaces logos despite preserving structure. In contrast, IMAGGarment-1 achieves accurate control over silhouette, color, and logo placement. On unseen garments, all baselines degrade notably. Subject-driven methods fail to generalize to novel layouts, AnyDoor distorts appearance, and BLIP-Diffusion struggles with logo positioning. Plugin-based methods also falter: ControlNet-Garment produces mismatched outputs, and IP-Adapter-Garment cannot interpret unseen spatial semantics. IMAGGarment-1 remains robust, maintaining alignment across all conditions. This generalization stems from our  $A^3$  module, which effectively integrates spatial and visual cues in the latent space. These results validate the controllability and flexibility of our method in both seen and unseen settings.

## 4.4 Ablations and Model Analysis

**Ablation of Architecture Design.** To validate the effectiveness of each component in our framework, we design a series of ablation variants within the IMAGGarment-1 architecture: **B0** uses the vanilla Stable Diffusion v1.5 without any of our proposed modules, serving as the baseline. **B1** removes the local enhancement model (Stage II), evaluating the impact of omitting logo injection and spatial control. **B2** removes the global appearance model (Stage

<sup>2</sup><https://huggingface.co/stable-diffusion-v1-5/stable-diffusion-v1-5>

<sup>3</sup><https://huggingface.co/stable-diffusion-v1-5/stable-diffusion-inpainting>

<sup>4</sup>[https://github.com/mlfoundations/open\\_clip](https://github.com/mlfoundations/open_clip)

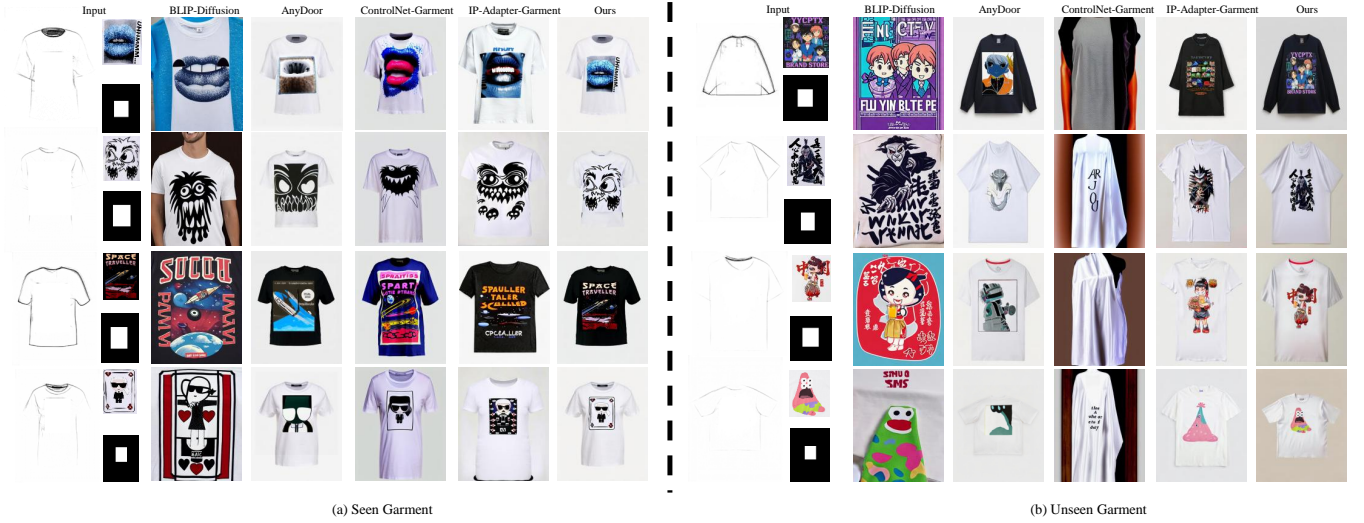


**Figure 5: Qualitative results on seen and unseen GarmentBench samples. The seen set uses original test pairs, while the unseen set involves randomly mixed conditions. IMAGGarment-1 delivers the most consistent outputs, achieving accurate silhouette, color, and logo control across both settings.**

**Table 2: Quantitative ablation results on GarmentBench.**

| Method      | FID ↓          | LPIPS ↓       | CSS ↓          | LLA ↑         | CLIPScore ↑   |
|-------------|----------------|---------------|----------------|---------------|---------------|
| B0          | 130.1314       | 0.6495        | 105.1591       | 0.1719        | 0.3476        |
| B1          | 44.2250        | 0.1633        | 34.4135        | 0.2997        | 0.3145        |
| B2          | 23.9822        | 0.3336        | 97.245         | 0.6099        | 0.3454        |
| B3          | 20.0446        | 0.1488        | 62.2521        | 0.6701        | 0.3413        |
| B4          | 37.8463        | 0.3881        | 101.8441       | 0.5780        | 0.3359        |
| <b>Full</b> | <b>11.7038</b> | <b>0.0904</b> | <b>33.1443</b> | <b>0.7336</b> | <b>0.3460</b> |

I), assessing the model’s performance without structured silhouette and color conditioning. **B3** removes the color adapter from the global appearance model, isolating the role of color guidance in generation. **B4** replaces our mixed attention with vanilla self-attention in the denoising UNet, testing the importance of spatial fusion with silhouette features. **Full** represents the complete IMAGGarment-1 framework with all proposed modules integrated.

Table 2 presents the quantitative impact of each component in our proposed IMAGGarment-1. In B1, which removes the local enhancement stage, the model struggles to place logos precisely, leading to degraded LLA and CLIPScore. Although the overall garment structure is preserved, the lack of spatial control prevents accurate logo integration. In B2, without the global appearance stage, the model fails to maintain silhouette and color consistency, resulting in significantly worse FID, LPIPS, and CSS. This demonstrates that local injection alone is insufficient to handle global garment layouts. B3 disables the color adapter, causing notable drops in CSS, highlighting its role in faithful color transfer and control. B4 replaces our mixed attention with standard self-attention, which weakens the fusion of silhouette guidance and causes drops in both LPIPS and FID, indicating reduced realism and structural coherence. The full IMAGGarment-1 achieves the best performance across all metrics, validating the complementary design of each module’s



**Figure 6: Qualitative ablation results on GarmentBench.**

effectiveness in handling multi-condition garment generation. Further, Figure 6 shows qualitative comparisons. B1 fails to align logos spatially, while B2 produces distorted garments lacking color and silhouette guidance. Despite maintaining logo placement, B3 leads to color mismatch, and B4 generates less coherent garment layouts. In contrast, the full model successfully synthesizes garments with accurate silhouettes, precise logo placement, and faithful color reproduction, demonstrating the benefits of our dual-stage design, color adapter, and mixed attention fusion.

**Controllability Analysis.** To evaluate the controllability of the proposed IMAGGarment-1, we conduct conditional manipulation experiments by varying one condition at a time, silhouette, color palette, or logo position, while keeping the others fixed. As shown in Figure 7, each two-row block highlights the model’s response to a specific condition. When changing the silhouette (top block), the





**Figure 7: Controllability visualization.** Each block varies one input condition while keeping others fixed. **Top: Silhouette changes lead to consistent structural adaptation.** **Middle: Color palette variation results in accurate color transfer.** **Bottom: Logo mask adjustment yields precise spatial placement.**

generated garments conform precisely to the target shapes, demonstrating the capability of the mixed attention module to preserve structural alignment. With color palette variation (middle block), the model consistently reproduces the desired color distributions, verifying the effectiveness of the color adapter in enabling color-faithful generation. Finally, adjusting the logo position (bottom block) yields accurate spatial relocation, highlighting the  $A^3$  module’s ability to inject spatial priors for precise local control. These results demonstrate that IMAGGarment-1 enables fine-grained, decoupled control over garment attributes, supporting practical and flexible generation for real-world fashion design applications.

**Hyperparameter Analysis.** We study the effect of two key hyperparameters in Eq. 1 and Eq. 3: the silhouette guidance weight  $\alpha$  and the color conditioning weight  $\beta$ . As shown in Figure 8, varying  $\alpha$  directly impacts the model’s ability to follow the reference silhouette. When  $\alpha$  is too low, the generated structure becomes blurry or deviates from the target shape; when too high, it may suppress color and text guidance. We empirically set  $\alpha = 0.6$  for a balanced structural alignment. Similarly, the color weight  $\beta$  controls



**Figure 8: Hyperparameter analysis of silhouette weight  $\alpha$  and color weight  $\beta$ .** Increasing  $\alpha$  improves structural alignment up to a point, while larger  $\beta$  enhances color fidelity.

the influence of the color palette. As  $\beta$  increases, color consistency improves steadily, with  $\beta = 1.0$  yielding visual fidelity performance. **Limitations.** While IMAGGarment-1 achieves strong performance in FGG, several limitations remain. First, the base diffusion model’s capability still constrains the visual quality and color fidelity of generated results. Incorporating stronger pre-trained backbones such as Stable Diffusion 3 [10] or Flux [22] could further enhance generation quality. Second, the current framework is limited to single-view, flat garment images. However, practical applications in fashion design often require dynamic visualization and 3D consistency. Addressing this requires high-quality multi-view or temporally aligned datasets, which we plan to explore to enable more expressive and realistic garment generation in future work. As Neil Armstrong once said, “*That’s one small step for a man, one giant leap for mankind.*” We hope this work marks a small but meaningful step toward the future of personalized fashion generation.

## 5 CONCLUSION

We propose IMAGGarment-1, a unified conditional diffusion framework for fine-grained garment generation with precise control over silhouette, color, and logo placement. By introducing mixed attention, color adapter, and the  $A^3$  module, our framework explicitly disentangles global structure (silhouette and color) from local attributes (logo content and spatial placement), enabling accurate spatial control and high-quality synthesis. To support this task, we construct GarmentBench, a large-scale benchmark with over 180K samples annotated with multi-level design conditions. Comprehensive experiments on both seen and unseen garments demonstrate that IMAGGarment-1 achieves state-of-the-art results in structure fidelity, color consistency, and logo controllability.





## REFERENCES

- [1] Jinze Bai, Shuai Bai, Shusheng Yang, Shijie Wang, Sinan Tan, Peng Wang, Junyang Lin, Chang Zhou, and Jingren Zhou. 2023. Qwen-VL: A Versatile Vision-Language Model for Understanding, Localization, Text Reading, and Beyond. *arXiv:2308.12966* [cs.CV] <https://arxiv.org/abs/2308.12966>
- [2] Caroline Chan, Frédo Durand, and Phillip Isola. 2022. Learning to generate line drawings that convey geometry and semantics. In *Proceedings of the IEEE/CVF Conference on Computer Vision and Pattern Recognition*. 7915–7925.
- [3] Shu-Yu Chen, Feng-Lin Liu, Yu-Kun Lai, Paul L. Rosin, Chunpeng Li, Hongbo Fu, and Lin Gao. 2021. DeepFaceEditing: deep face generation and editing with disentangled geometry and appearance control. *ACM Trans. Graph.* 40, 4, Article 90 (July 2021), 15 pages. <https://doi.org/10.1145/3450626.3459760>
- [4] Shu-Yu Chen, Wanchao Su, Lin Gao, Shihong Xia, and Hongbo Fu. 2020. DeepFaceDrawing: deep generation of face images from sketches. *ACM Trans. Graph.* 39, 4, Article 72 (Aug. 2020), 16 pages. <https://doi.org/10.1145/3386569.3392386>
- [5] Weifeng Chen, Tao Gu, Yuhao Xu, and Arlene Chen. 2024. Magic clothing: Controllable garment-driven image synthesis. In *Proceedings of the 32nd ACM International Conference on Multimedia*. 6939–6948.
- [6] Wengling Chen and James Hays. 2018. Sketchygan: Towards diverse and realistic sketch to image synthesis. In *Proceedings of the IEEE conference on computer vision and pattern recognition*. 9416–9425.
- [7] Xi Chen, Lianghua Huang, Yu Liu, Yujun Shen, Deli Zhao, and Hengshuang Zhao. 2024. Anydoor: Zero-shot object-level image customization. In *Proceedings of the IEEE/CVF conference on computer vision and pattern recognition*. 6593–6602.
- [8] Yuanzheng Ci, Xinzhu Ma, Zhihui Wang, Haojie Li, and Zhongxuan Luo. 2018. User-Guided Deep Anime Line Art Colorization with Conditional Adversarial Networks. In *Proceedings of the 26th ACM International Conference on Multimedia (Seoul, Republic of Korea) (MM '18)*. Association for Computing Machinery, New York, NY, USA, 1536–1544. <https://doi.org/10.1145/3240508.3240661>
- [9] Antonia Creswell, Tom White, Vincent Dumoulin, Kai Arulkumaran, Biswa Sengupta, and Anil A Bharath. 2018. Generative adversarial networks: An overview. *IEEE signal processing magazine* 35, 1 (2018), 53–65.
- [10] Patrick Esser, Sumith Kulal, Andreas Blattmann, Rahim Entezari, Jonas Müller, Harry Saini, Yam Levi, Dominik Lorenz, Axel Sauer, Frederic Boesel, et al. 2024. Scaling rectified flow transformers for high-resolution image synthesis. In *Forty-first international conference on machine learning*.
- [11] Masato Fujitake. 2024. RL-logo: Deep reinforcement learning localization for logo recognition. In *ICASSP 2024-2024 IEEE International Conference on Acoustics, Speech and Signal Processing (ICASSP)*. IEEE, 2830–2834.
- [12] Junyao Gao, Yanan Sun, Fei Shen, Xin Jiang, Zhening Xing, Kai Chen, and Cairong Zhao. 2025. Faceshot: Bring any character into life. *arXiv preprint arXiv:2503.00740* (2025).
- [13] Arnab Ghosh, Richard Zhang, Puneet K Dokania, Oliver Wang, Alexei A Efros, Philip HS Torr, and Eli Shechtman. 2019. Interactive sketch & fill: Multiclass sketch-to-image translation. In *Proceedings of the IEEE/CVF International Conference on Computer Vision*. 1171–1180.
- [14] Kaiming He, Xiangyu Zhang, Shaoqing Ren, and Jian Sun. 2015. Deep Residual Learning for Image Recognition. *arXiv:1512.03385* [cs.CV] <https://arxiv.org/abs/1512.03385>
- [15] Jack Hessel, Ari Holtzman, Maxwell Forbes, and Yejin Choi. 2021. CLIPScore: A Reference-free Evaluation Metric for Image Captioning. In *Proceedings of the 2021 Conference on Empirical Methods in Natural Language Processing (EMNLP)*. 7514–7528.
- [16] Martin Heusel, Hubert Ramsauer, Thomas Unterthiner, Bernhard Nessler, and Sepp Hochreiter. 2017. Gans trained by a two time-scale update rule converge to a local nash equilibrium. *Advances in neural information processing systems* 30 (2017).
- [17] Jonathan Ho, Ajay Jain, and Pieter Abbeel. 2020. Denoising diffusion probabilistic models. In *NeurIPS*.
- [18] Jonathan Ho and Tim Salimans. 2022. Classifier-free diffusion guidance. *arXiv preprint arXiv:2207.12598* (2022).
- [19] Phillip Isola, Jun-Yan Zhu, Tinghui Zhou, and Alexei A Efros. 2017. Image-to-image translation with conditional adversarial networks. In *Proceedings of the IEEE conference on computer vision and pattern recognition*. 1125–1134.
- [20] Glenn Jocher, Jing Qiu, and Ayush Chaurasia. 2023. Ultralytics YOLO. <https://github.com/ultralytics/ultralytics>
- [21] Taewook Kim, Ze Wang, Zhengyuan Yang, Jiang Wang, Lijuan Wang, Zicheng Liu, and Qiang Qiu. 2024. Conditional Text-to-Image Generation with Reference Guidance. *arXiv preprint arXiv:2411.16713* (2024).
- [22] Black Forest Labs. 2024. FLUX. <https://github.com/black-forest-labs/flux>.
- [23] Dongxu Li, Junnan Li, and Steven Hoi. 2023. Blip-diffusion: Pre-trained subject representation for controllable text-to-image generation and editing. *Advances in Neural Information Processing Systems* 36 (2023), 30146–30166.
- [24] Zeyu Li, Cheng Deng, Erkun Yang, and Dacheng Tao. 2020. Staged sketch-to-image synthesis via semi-supervised generative adversarial networks. *IEEE Transactions on Multimedia* 23 (2020), 2694–2705.
- [25] Ente Lin, Xujie Zhang, Fuwei Zhao, Yuxuan Luo, Xin Dong, Long Zeng, and Xiaodan Liang. 2024. DreamFit: Garment-Centric Human Generation via a Lightweight Anything-Dressing Encoder. *arXiv preprint arXiv:2412.17644* (2024).
- [26] Yaron Lipman, Ricky TQ Chen, Heli Ben-Hamu, Maximilian Nickel, and Matt Le. 2022. Flow matching for generative modeling. *arXiv preprint arXiv:2210.02747* (2022).
- [27] Yifan Liu, Zengchang Qin, Zhenbo Luo, and Hua Wang. 2017. Auto-painter: Cartoon image generation from sketch by using conditional generative adversarial networks. *arXiv preprint arXiv:1705.01908* (2017).
- [28] Ilya Loshchilov and Frank Hutter. 2019. Decoupled Weight Decay Regularization. *arXiv:1711.05101* [cs.LG] <https://arxiv.org/abs/1711.05101>
- [29] Liqian Ma, Xu Jia, Qianru Sun, Bernt Schiele, Tinne Tuytelaars, and Luc Van Gool. 2017. Pose guided person image generation. In *NeurIPS*.
- [30] J. MacQueen. 1967. Some Methods for Classification and Analysis of Multivariate Observations. In *Proceedings of the Fifth Berkeley Symposium on Mathematical Statistics and Probability, Volume 1: Statistics*. University of California Press, 281–297.
- [31] Yifang Men, Yiming Mao, Yuning Jiang, Wei-Ying Ma, and Zhouhui Lian. 2020. Controllable person image synthesis with attribute-decomposed gan. In *Proceedings of the IEEE/CVF conference on computer vision and pattern recognition*. 5084–5093.
- [32] Mehdi Mirza and Simon Osindero. 2014. Conditional generative adversarial nets. *arXiv preprint arXiv:1411.1784* (2014).
- [33] Dustin Podell, Zion English, Kyle Lacey, Andreas Blattmann, Tim Dockhorn, Jonas Müller, Joe Penna, and Robin Rombach. 2023. Sdxl: Improving latent diffusion models for high-resolution image synthesis. *arXiv preprint arXiv:2307.01952* (2023).
- [34] Robin Rombach, Andreas Blattmann, Dominik Lorenz, Patrick Esser, and Björn Ommer. 2022. High-resolution image synthesis with latent diffusion models. In *Proceedings of the IEEE/CVF conference on computer vision and pattern recognition*. 10684–10695.
- [35] Fei Shen, Xin Jiang, Xin He, Hu Ye, Cong Wang, Xiaoyu Du, Zechao Li, and Jinhui Tai. 2024. Imadressing-v1: Customizable virtual dressing. *arXiv preprint arXiv:2407.12705* (2024).
- [36] Aliaksandr Siarohin, Enver Sangineto, Stéphane Lathuilière, and Nicu Sebe. 2018. Deformable gans for pose-based human image generation. In *Proceedings of the IEEE conference on computer vision and pattern recognition*. 3408–3416.
- [37] Jiaming Song, Chenlin Meng, and Stefano Ermon. 2022. Denoising Diffusion Implicit Models. *arXiv:2010.02502* [cs.LG] <https://arxiv.org/abs/2010.02502>
- [38] Yang Song, Jascha Sohl-Dickstein, Diederik P Kingma, Abhishek Kumar, Stefano Ermon, and Ben Poole. 2020. Score-based generative modeling through stochastic differential equations. *arXiv preprint arXiv:2011.13456* (2020).
- [39] Andrey Voynov, Kfir Aberman, and Daniel Cohen-Or. 2023. Sketch-guided text-to-image diffusion models. In *ACM SIGGRAPH 2023 conference proceedings*. 1–11.
- [40] Xian Wu, Chen Wang, Hongbo Fu, Ariel Shamir, Song-Hai Zhang, and Shi-Min Hu. 2022. DeepPortraitDrawing: Generating Human Body Images from Freehand Sketches. *arXiv:2205.02070* [cs.CV] <https://arxiv.org/abs/2205.02070>
- [41] Yuhao Xu, Tao Gu, Weifeng Chen, and Chengcai Chen. 2024. Ootdiffusion: Outfitting fusion based latent diffusion for controllable virtual try-on. *arXiv preprint arXiv:2403.01779* (2024).
- [42] Hu Ye, Jun Zhang, Sibio Liu, Xiao Han, and Wei Yang. 2023. Ip-adapter: Text compatible image prompt adapter for text-to-image diffusion models. *arXiv preprint arXiv:2308.06721* (2023).
- [43] Kai Zeng, Zhou Wang, Anmin Zhang, Zhaohui Wang, and Wenjun Zhang. 2014. A color structural similarity index for image quality assessment. In *2014 IEEE International Conference on Image Processing (ICIP)*. IEEE, 660–664. <https://doi.org/10.1109/ICIP.2014.7025894>
- [44] Jinghao Zhang, Wen Qian, Hao Luo, Fan Wang, and Feng Zhao. 2024. AnyLogo: Symbiotic Subject-Driven Diffusion System with Gemini Status. *arXiv preprint arXiv:2409.17740* (2024).
- [45] Lvmin Zhang, Anyi Rao, and Maneesh Agrawala. 2023. Adding conditional control to text-to-image diffusion models. In *Proceedings of the IEEE/CVF international conference on computer vision*. 3836–3847.
- [46] Richard Zhang, Phillip Isola, Alexei A Efros, Eli Shechtman, and Oliver Wang. 2018. The unreasonable effectiveness of deep features as a perceptual metric. In *Proceedings of the IEEE conference on computer vision and pattern recognition*. 586–595.
- [47] Xujie Zhang, Binbin Yang, Michael C Kampffmeyer, Wenqing Zhang, Shiyue Zhang, Guansong Lu, Liang Lin, Hang Xu, and Xiaodan Liang. 2023. Diffcloth: Diffusion based garment synthesis and manipulation via structural cross-modal semantic alignment. In *Proceedings of the IEEE/CVF International Conference on Computer Vision*. 23154–23163.
- [48] Mingkang Zhu, Xi Chen, Zhongdao Wang, Hengshuang Zhao, and Jiaya Jia. 2024. LogoSticker: Inserting Logos Into Diffusion Models for Customized Generation. In *European Conference on Computer Vision*. Springer, 363–378.

## SUPPLEMENTARY MATERIAL

This supplementary material provides additional details and discussions to support the findings in the main paper. Section A introduces key notations and symbol definitions used throughout the paper. Section B explains the evaluation metrics, including their motivations and computational formulas. Section C presents an ethics statement discussing the potential risks and responsible use of our method. Section D includes extended results, such as more controllability visualization and more qualitative.

### A SOME NOTATIONS AND DEFINITIONS

**Table 3: Some notations and definitions.**

| Notation           | Definition                          |
|--------------------|-------------------------------------|
| $t$                | Timestep                            |
| $Z_t$              | Latent feature at $t$ step          |
| $Z_m$              | Output of mixed attention           |
| $x_0$              | Real image                          |
| $x_t$              | Noisy data at $t$ step              |
| $G$                | Garment image                       |
| $L$                | Logo image                          |
| $M$                | Mask image                          |
| $C_g$              | Feature of garment image            |
| $C_l$              | Feature of logo image               |
| $C_m$              | Feature of mask image               |
| $C_s$              | Feature of silhouette image         |
| $C_c$              | Feature of color image              |
| $C_t$              | Feature of text prompt              |
| $\tilde{I}_c$      | Generated garment image             |
| $\theta$           | Diffusion model                     |
| $\epsilon$         | Gaussian noise                      |
| $\tilde{\alpha}_t$ | Cumulative product of noise weights |
| $w$                | Guidance scale                      |
| $\alpha$           | Silhouette scale                    |
| $\beta$            | Color scale                         |

### B EVALUATION METRICS

We employ five quantitative metrics to evaluate the performance of our method with respect to visual quality, structural and semantic consistency, and controllability. All metrics are computed between the generated image  $I_{\text{gen}}$  and its corresponding ground truth  $I_{\text{gt}}$ , given a shared input condition set.

**Fréchet Inception Distance (FID)** [16] measures the distribution-level similarity between generated and real images in the feature space of an Inception-V3 network. Let  $(\mu_r, \Sigma_r)$  and  $(\mu_g, \Sigma_g)$  denote the means and covariances of the real and generated image features, respectively. The metric is calculated as:

$$\text{FID} = \|\mu_r - \mu_g\|_2^2 + \text{Tr}(\Sigma_r + \Sigma_g - 2(\Sigma_r \Sigma_g)^{1/2}). \quad (12)$$

**Learned Perceptual Image Patch Similarity (LPIPS)** [46] evaluates perceptual similarity between  $I_{\text{gen}}$  and  $I_{\text{gt}}$  using deep features from a pretrained network (AlexNet). Let  $f^l(I)$  be the activation at layer  $l$  and location  $(h, w)$ , and  $w^l$  be a learned per-layer weight.

LPIPS is computed as:

$$\text{LPIPS}(I_{\text{gen}}, I_{\text{gt}}) = \sum_l \frac{1}{H_l W_l} \sum_{h,w} \|w^l \odot (f_{h,w}^l(I_{\text{gen}}) - f_{h,w}^l(I_{\text{gt}}))\|_2^2. \quad (13)$$

**Color Structure Similarity (CSS)** [43] measures the distance between the generated and reference color palettes. Given palettes  $P_{\text{gen}}$  and  $P_{\text{gt}}$  with  $K$  dominant colors extracted via K-means clustering, CSS is defined as:

$$\text{CSS} = \frac{1}{K} \sum_{i=1}^K \|p_{\text{gen}}^{(i)} - p_{\text{gt}}^{(i)}\|_2. \quad (14)$$

**Logo Location Accuracy (LLA)** [11] quantifies the spatial deviation between the predicted and ground truth logo positions. Let  $\text{Rec}_{\text{gen}}$  and  $\text{Rec}_{\text{gt}}$  denote the rectangular areas of the logo in  $I_{\text{gen}}$  and  $I_{\text{gt}}$ , respectively. The metric is computed as:

$$\text{LLA} = \frac{\text{Intersection}(\text{Rec}_{\text{gen}}, \text{Rec}_{\text{gt}})}{\text{Union}(\text{Rec}_{\text{gen}}, \text{Rec}_{\text{gt}})}. \quad (15)$$

**CLIPScore** [15] evaluates semantic alignment between the generated image and the input text prompt  $T$ . Let  $f_{\text{img}}(\cdot)$  and  $f_{\text{text}}(\cdot)$  be CLIP encoders for images and text. The metric is defined as the cosine similarity:

$$\text{CLIPScore} = \cos(f_{\text{img}}(I_{\text{gen}}), f_{\text{text}}(T)). \quad (16)$$

Together, these metrics enable a rigorous and holistic assessment of fine-grained garment generation, covering realism, structure, color fidelity, spatial precision, and semantic consistency.

### C ETHICS STATEMENT

This work introduces IMAGGarment-1, a controllable multi-stage diffusion framework for fine-grained garment image generation. While our method is developed to support applications such as personalized fashion design and virtual try-ons, we acknowledge potential ethical risks. In particular, the ability to manipulate real person images could be misused to generate deceptive or unauthorized content. Many human-centric image synthesis techniques share such concerns. To mitigate misuse, we advocate for responsible research and deployment practices. Our method is intended for academic and design-oriented purposes, and we encourage the use of detection, attribution, and content moderation tools alongside generative models. We believe that IMAGGarment-1’s contribution advances the field in a meaningful and controllable direction, and we support community efforts to ensure its safe and ethical use.

### D ADDITIONAL RESULTS

**More Controllability Visualization.** Figure 9 provides additional visualizations of IMAGGarment-1’s controllability. These examples include challenging garment types such as textured tops, denim jeans, and skirts, further validating the model’s ability to achieve fine-grained and decoupled control over diverse attributes.

**More Qualitative Results for IMAGGarment-1.** Figure 10 displays additional results synthesized by IMAGGarment-1, demonstrating its robustness and high-quality garment generation across diverse test cases.



Figure 9: Controllability visualization of IMAGGarment-1. Each block varies one input condition while keeping others fixed. Top: Silhouette changes lead to consistent structural adaptation. Bottom: Color palette variation results in accurate color transfer. Examples include complex textures, denim, and skirts, demonstrating robustness across diverse garment types.

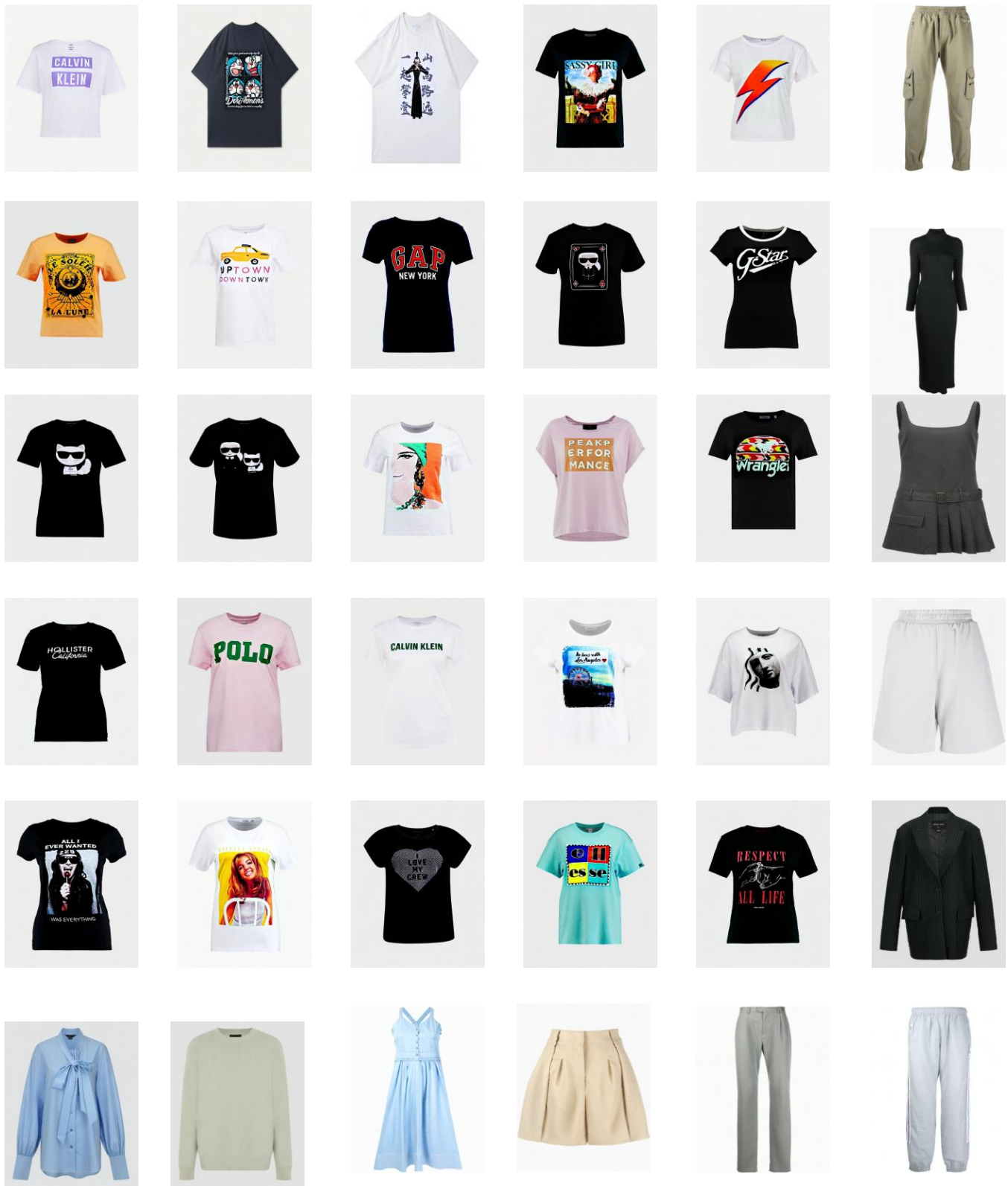


Figure 10: Additional qualitative results of IMAGGarment-1, demonstrating its robustness and visual fidelity across diverse garment styles and scenarios.